RESEARCH ARTICLE
PLANETARY SCIENCES

Earth and Planetary Physics
9: 1135–1146, 2025
doi: 10.26464/epp2025071

The KREEP-rich circum-Lalande region: A candidate landing area for future lunar crewed missions

Sheng Gou[1,2,3], ZongYu Yue[1,4], YangTing Lin[1]*, KaiChang Di[2,4], YuYang He[1], HengCi Tian[1], Patrick C. Pinet[5], ZhanChuan Cai[3], Roberto Bugiolacchi[3,6], HongLei Lin[1], Sen Hu[1], and Wei Yang[1]

[1]Key Laboratory of Planetary Science and Frontier Technology, Institute of Geology and Geophysics, Chinese Academy of Sciences, Beijing 100029, China;

[2]State Key Laboratory of Remote Sensing and Digital Earth, Aerospace Information Research Institute, Chinese Academy of Sciences, Beijing 100101, China;

[3]State Key Laboratory of Lunar and Planetary Sciences, Macau University of Science and Technology, Macao 999078, China;

[4]Center for Excellence in Comparative Planetology, Chinese Academy of Sciences, Hefei 230026, China;

[5]Institut de Recherche en Astrophysique et Planétologie, Université de Toulouse, Centre National de la Recherche Scientifique (CNRS), Université Paul Sabatier (UPS), Centre National D'Etudes Spatiales (CNES), Université de Toulouse III (UT3), Toulouse 44346, France;

[6]Earth Sciences, University College London, London WC1E 6BT, UK

Key Points:

- Candidate lunar landing sites are situated on the KREEP (potassium–rare earth element–phosphorus)–rich circum-Lalande region in the mare basalts.
- Extravehicular activities, such as collecting KREEP-rich materials, screening clast samples, and drilling regolith cores, are proposed for the astronauts.
- Samples are vital for exploring primordial KREEP, refining the lunar chronology, and studying volcanism and volatiles.

Citation: Gou, S., Yue, Z. Y., Lin, Y. T., Di, K. C., He, Y. Y., Tian, H. C., Pinet, P. C., Cai, Z. C., Bugiolacchi, R., … Yang, W. (2025). The KREEP-rich circum-Lalande region: A candidate landing area for future lunar crewed missions. *Earth Planet. Phys.*, *9*(6), 1135–1146. http://doi.org/10.26464/epp2025071

Abstract: The lunar magma ocean hypothesis suggests that the primordial KREEP (an acronym of potassium (K), rare earth element (REE), and phosphorus (P)) was the final product of fractional crystallization. However, the primordial KREEP (a.k.a. urKREEP) has never been identified in previous lunar samples or meteorites. The Moon is the focus of many countries' and agencies' space exploration plans, and with the advancement of technology, crewed missions have been proposed. We propose two candidate landing sites, located respectively in the northwest (9.5°W, 0.9°S) and southeast (11.1°W, 6.2°S) of Lalande crater (8.6°W, 4.5°S), for future crewed missions, with the primary goal of sampling the speculated urKREEP. Both sites are situated on the Th- (a critical marker of KREEP) and silica-rich Lalande ejecta in the Mare Insularum and Mare Nubium, respectively. Their geolocations at the low latitude on the lunar nearside, the flat surface, and the low rock abundance suggest the sites are safe for landing and meet the needs of real-time Earth–Moon communication. The astronauts could perform many extravehicular activities, such as collecting KREEP-rich samples, screening clast samples, and drilling regolith cores, to gather a variety of samples, such as Lalande ejecta, basalts, Copernicus ejecta, and regolith. The returned samples are valuable to explore the speculated urKREEP, to reveal the relationship between heat-producing elements and volcanism, to refine the lunar cratering chronology function, and to investigate volatiles in the regolith.

Keywords: primordial KREEP; Th-rich Lalande ejecta; landing sites; lunar crewed missions; extravehicular activities

1. Introduction

The lunar magma ocean (LMO) hypothesis is the basis for understanding the formation and evolution of the Moon and terrestrial planets. This hypothesis suggests that the Moon was once globally molten, then underwent fractional crystallization and formed the lunar mantle and crust (Smith et al., 1970; Wood et al., 1970). During the late stage of LMO evolution (≥99% crystallization), the residual magma became enriched in potassium (K), rare earth elements (REEs), and phosphorus (P) (collectively referred to as KREEP), as well as iron (Fe), titanium (Ti), thorium (Th), and other incompatible elements. This process led to the formation of a KREEP-rich reservoir (termed primordial KREEP or urKREEP) and ilmenite-bearing cumulates (Hubbard et al., 1971; Warren and Wasson, 1979; Moriarty et al., 2021). The radioactive heat-producing elements (HPEs), such as Th and K, which are enriched within the urKREEP and emit gamma rays continuously and spontaneously, are proposed to sustain prolonged magmatic activity through radiogenic heating (Haskin et al., 2000; Wieczorek and

First author: S. Gou, gousheng@mail.iggcas.ac.cn
Correspondence to: Y. T. Lin, linyt@mail.iggcas.ac.cn
Received 19 FEB 2025; Accepted 30 APR 2025.
First Published online 11 JUN 2025.

Phillips, 2000; Borg et al., 2004). The enrichment of KREEP components in lunar rocks appears to be closely tied to the geochemical evolution of the urKREEP (Warren and Wasson, 1979). The HPEs–KREEP coupling relation suggests the potential distribution of KREEP on the lunar surface could be investigated by mapping surficial HPEs with gamma-ray spectrometry from spacecraft in lunar orbit. The Lunar Prospector (LP) gamma-ray spectrometer (GRS) revealed that the lunar surface has distinct chemical element variations (Lawrence et al., 1998). The hot spots with the highest Th and K abundances are primarily concentrated in the nearside, particularly in the Oceanus Procellarum region, namely, the Procellarum KREEP Terrane (PKT; Jolliff et al., 2000; Figure 1).

The KREEP component was first discovered in Apollo 12 samples (Meyer et al., 1971). Because of its unique chemical composition and formation mechanism, KREEP is considered an important target for deciphering the geochemical and thermal evolution of the Moon, as well as for determining the lunar lithologies and terranes (Warren and Wasson, 1979; Jolliff et al., 2000; Levin et al., 2025). For example, KREEP-induced melting was proposed to be responsible for the mare floodings in the PKT (Haskin et al., 2000). However, many challenges and questions remain regarding KREEP:

(1) The formation of KREEP involves a variety of complex geological processes and chemical reactions, leading to a complex interpretation of the abundance of incompatible elements. For instance, Chang'e-5 samples suggest that the Th anomaly (~4.5 ppm) in the basalts is due to low-degree partial melting and extensive fractional crystallization, which does not necessarily correlate with KREEP-rich lithologies (Tian HC et al., 2021). This finding challenges the presumed HPEs–KREEP coupling hypothesis in lunar evolution. Additionally, a rather low Th content of ~0.9 ppm in the Chang'e-6 basalt samples indicates that KREEP components contributed little to the magma eruption in the sampling region (Cui ZX et al., 2024; Li CL et al., 2024; Zhang QWL et al., 2024).

(2) The speculated urKREEP has not been sampled in any missions or meteorites, preventing an in-depth understanding of the LMO hypothesis and making sampling of urKREEP materials a priority to constrain its putative existence. For example, only a few urKREEP-like lithic clasts or impact melt breccias were reported in Apollo samples (Warren and Wasson, 1979; Liu DY et al., 2012) and in the Sayh al Uhaymir (SaU) 169 lunar meteorite (Gnos et al., 2004; Lin Y et al., 2012).

(3) The lateral and vertical extent of the urKREEP is still under debate, and several mechanisms have been proposed to explain the observed asymmetric distribution of the patchy KREEP-related materials, such as inhomogeneous differentiation (Parmentier et al., 2002; Wieczorek et al., 2006) and antipodal impact effects (Schultz and Crawford, 2011; Zhang N et al., 2022).

(4) The number of returned KREEP-rich samples is relatively small and they could be from specific regions, preventing researchers from conducting comprehensive studies on their character and origin. For example, Meyer et al. (1971) proposed that the KREEP components in Apollo 15 samples might have originated from the Imbrian basin and represent an important component of the pre-mare crust.

The above-mentioned challenges and questions highlight the urgent need for more KREEP-rich samples, especially those from unexplored areas, to provide clues to the formation, distribution, and composition of the hypothesized urKREEP (National Research Council, 2007). In addition, REEs and P in the KREEP are potential targets for future *in situ* resource utilization. Many countries and agencies have already proposed a series of lunar missions, such as the United States' Artemis program (Smith et al., 2020), China's lunar exploration project (Wu YH, 2023), Russia's Luna mission (Mitrofanov et al., 2021), India's Chandrayaan program (Palanivel,

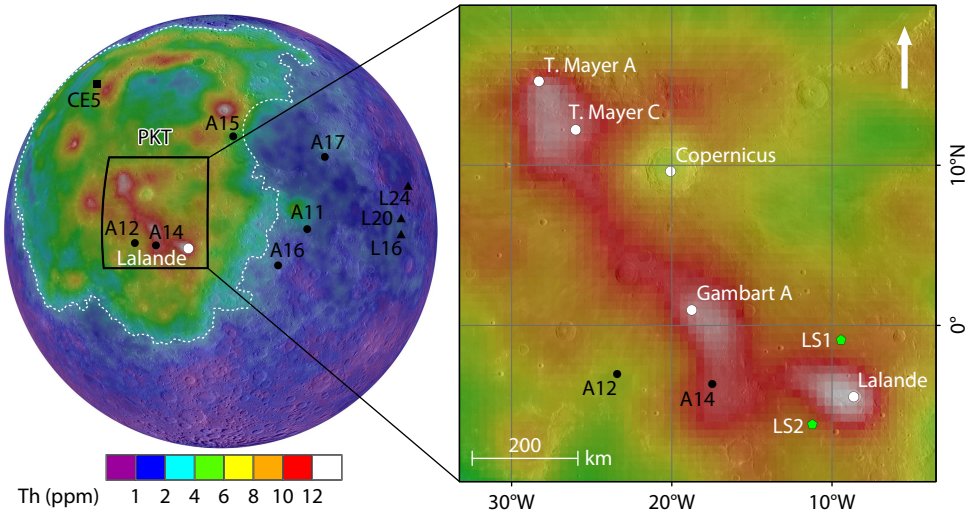

Figure 1. Context of Th abundance in the circum-Lalande region (Lawrence et al., 1998). The dashed white line outlines the approximate extent of the Procellarum KREEP Terrane (PKT; Jolliff et al., 2000). The Lalande, Gambart A, T. Mayer A, and T. Mayer C craters have the highest Th contents (~13 ppm) exposed. Copernicus represents an anchor crater in the lunar cratering chronology. The previous Apollo (A), Luna (L), and Chang'e (CE) sampling missions are shown to provide a clear depiction of the distribution of prior sampling sites. LS1 and LS2 are the candidate landing sites proposed for future crewed missions (see Section 4.1).

2024), and the European Space Agency's Argonaut mission (Cifani et al., 2024). According to China's deep space exploration plan (Wu YH, 2023), the Moon will be the focus in the next 10 years. A set of upcoming robotic missions are planned for 2026 and beyond to explore the Moon's south pole, namely, Chang'e-7, Chang'e-8, and the International Lunar Research Station (Wu YH, 2023; Wang C et al., 2024). Additionally, China has planned missions to achieve a crewed lunar landing before 2030 (Wu YH, 2023), and potential landing sites have been proposed based on scientific values, such as the enigmatic Irregular Mare Patches in the Ina, the mysterious bright Reiner Gamma swirl, and the Aristarchus plateau, which has diverse geological features (Niu R et al., 2023). Since the Apollo 17 first landed on the lunar surface in 1972, human beings have not returned to the Moon in the last 53 years. Crewed missions to the Moon and other planets are dangerous; however, the risks have decreased substantially with the advancement of technology. Although both robotic and crewed missions have technological, social, and scientific benefits, the crewed ones have their own advantages. For example, the astronauts can make real-time decisions and perform extravehicular activities (EVAs) to increase mission efficiency. And even though KREEP components hold important clues for deciphering lunar geochemical and thermal evolution, none of the previous lunar missions have explicitly prioritized the collection of KREEP-rich materials as a primary scientific objective. To address this gap, in the present study we propose the KREEP-rich regions on the lunar surface as candidate landing areas for sample return in future missions.

The global distribution of Th (min: ~0 ppm, max: ~13 ppm) suggests the KREEP materials are enriched in the southeast of the PKT (Figure 1). Specifically, the vicinities of the Lalande (8.65°W, 4.46°S, 23.5 km), Gambart A (18.76°W, 0.96°N, 11.6 km), T. Mayer A (28.3°W, 15.2°N, 16.2 km), and T. Mayer C (26.0°W, 12.2°N, 14.9 km) craters have Th abundances as high as ~13 ppm. The empirical relationship between crater diameter and excavation depth (Melosh, 1989) suggests the Lalande crater is capable of exposing materials at greater depth (down to ~2.2 km). The Th-rich Lalande ejecta are thus ideal proxies for exploring the patchy nature and vertical extent of the urKREEP. To collect KREEP-rich samples with certainty, we propose the circum-Lalande region in this study as a potential landing area for future crewed missions. Using diverse datasets and products, especially those acquired over the last three decades, we describe the geological context of the circum-Lalande region and scientific problems related to samples from this region in the following sections. We also propose candidate landing sites and EVAs for the astronauts with the aim of maximizing scientific outcomes.

2. Data

Multiple datasets and products from several missions (Table 1) were used to explore the geological context of the KREEP-rich circum-Lalande region. The Lunar Reconnaissance Orbiter Camera (LROC) Wide Angle Camera (WAC) global mosaic (Speyerer et al., 2011) and Narrow Angle Camera (NAC) images (Robinson et al., 2010) were used for the morphology investigation. The TiO_2 abundance map generated from the WAC ultraviolet and visible images (Sato et al., 2017), the Mg number (Mg#), and mineral abundance maps produced from the Kaguya Multiband Imager (MI) data (Lemelin et al., 2016; Zhang L et al., 2023), the elemental maps (especially Th) derived from the LP GRS data (Lawrence et al., 1998), and the Christiansen feature (CF) map derived from the Lunar Reconnaissance Orbiter (LRO) Diviner Radiometer data (Greenhagen et al., 2010) were used for compositional interpretation. The blended digital terrain model (DEM), known as SLDEM2015, generated from the Lunar Orbiter Laser Altimeter (LOLA) altimetric profiles and the Kaguya Terrain Camera (TC) stereo images (Barker et al., 2016), and the LRO Diviner-derived rock abundance (RA) map (Powell et al., 2023) were used for topography examination and safety assessment of the potential landing sites.

3. Geological Context of the Circum-Lalande Region

3.1 Lalande and Copernicus Craters

Lalande crater (center location: 8.6°W, 4.5°S; diameter: ~23.5 km) is a Copernican-aged crater that has a sharp rim and an obvious ray system (Li B et al., 2018; Figure 2). It was formed in the lunar highlands and lies at the eastern edge of Mare Insularum and the northern border of Mare Nubium (Figure 2a). Low-relief bulges, which may be the impact melt products, are found on the floor of Lalande crater (Li B et al., 2018). The Th abundance and CF maps (Lawrence et al., 1998; Greenhagen et al., 2010) reveal that Lalande crater and its ejecta feature high Th (~12.9 ppm; Figure 2b) and silicic materials (CF value: ~7.8 μm; Figure 2c).

Table 1. List of datasets and products used for the geological context description.

Purpose	Product	Resolution	Data source	Reference
Morphology investigation	WAC mosaic	100 m/pixel	LROC WAC	Speyerer et al. (2011)
	NAC images	0.5–2.0 m/pixel	LROC NAC	Robinson et al. (2010)
Compositional interpretation	TiO_2 map	400 m/pixel	LROC WAC	Sato et al. (2017)
	Mg# map	512 pixel/degree	Kaguya MI	Zhang L et al. (2023)
	Elemental maps	2 pixel/degree	LP GRS	Lawrence et al. (1998)
	Mineral maps	512 pixel/degree	Kaguya MI	Lemelin et al. (2016)
	CF map	128 pixel/degree	LRO Diviner	Greenhagen et al. (2010)
Topography examination and safety assessment	SLDEM2015	512 pixel/degree	LRO LOLA & Kaguya TC	Barker et al. (2016)
	RA map	128 pixel/degree	LRO Diviner	Powell et al. (2023)

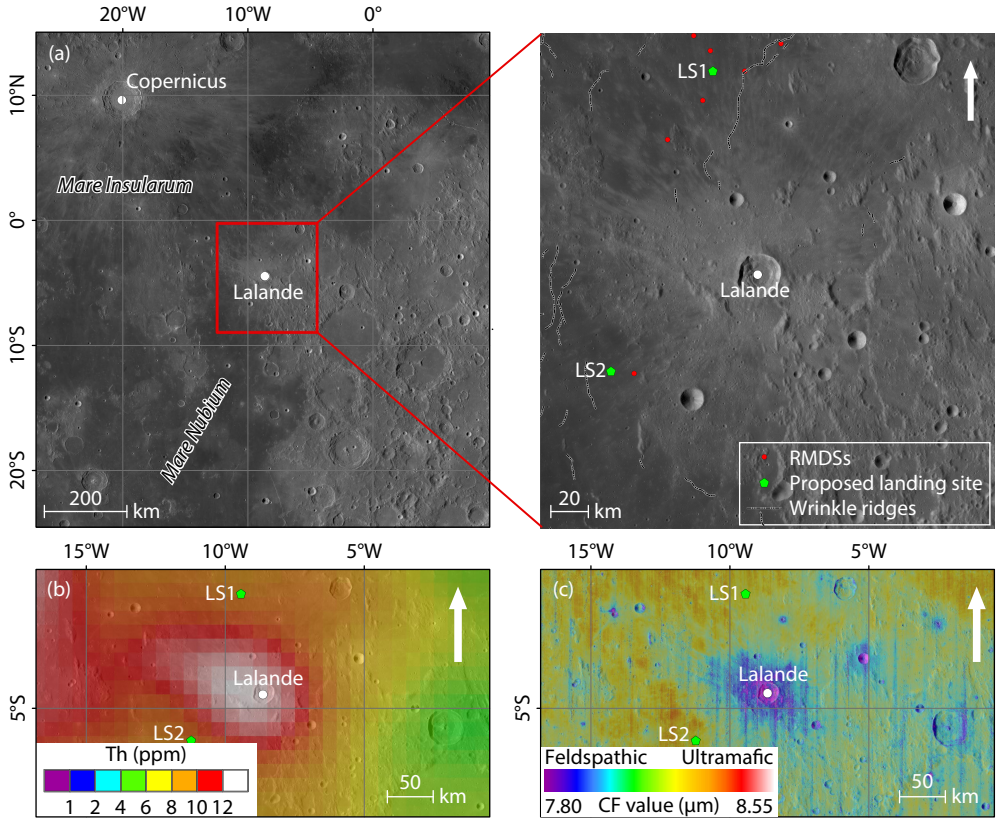

Figure 2. Context of the circum-Lalande region. (a) WAC image (Speyerer et al., 2011). The zoomed image shows Lalande's striking ray system. Wrinkle ridges and ring-moat dome structures (RMDSs) are typical landforms in the circum-Lalande region (see Section 3.4). The wrinkle ridges were identified by Thompson et al. (2017), and the RMDSs were identified from LROC NAC images (Robinson et al., 2010) in this study. LS1 and LS2 are the candidate landing sites proposed for future crewed missions (see Section 4.1). (b) Th-rich anomaly (Lawrence et al., 1998). (c) Silica-rich anomaly (Greenhagen et al., 2010).

Copernicus crater (center location: 20.1°W, 9.6°N; diameter: ~96.1 km) is another Copernican-aged crater in this region. Theoretically, it would excavate deeper than the Lalande (Melosh, 1989) and would expose KREEP-rich materials if the urKREEP distributed homogeneously (Warren and Wasson, 1979). However, the Th abundance map (Lawrence et al., 1998) reveals that the area surrounding the Copernicus crater is relatively Th-poor (Figure 1). Because the impact that formed a crater would pulverize and eject boulders to tens of kilometers away, the ejecta of the two fresh rayed craters may have deposited successively in the same area. Therefore, it is very likely that the materials excavated by the Lalande and Copernicus could be collected at the same time if a candidate landing site were chosen carefully.

3.2 Mare Insularum

The Mare Insularum (center location: 30.6°W, 7.8°N) is located in the pre-Nectarian-aged Insularum basin, which has rings of ~600 km and ~1000 km in diameter (Wilhelms and McCauley, 1971; Figure 3a). It covers an area of ~900 km in diameter and is bordered by the Kepler crater on the west, Sinus Aestuum on the east, and Montes Carpatus on the north, and it merges into Mare Cognitum on the south. Large parts of the Mare Insularum are influenced by the ejecta rays of Copernicus and Lalande craters (Figure 3).

The Insularum basin was flooded by multiple volcanic activities, as illustrated by various TiO_2 abundances in the mare basalts (Sato et al., 2017; Figure 3b). Hiesinger et al. (2011) conducted crater size–frequency distribution measurements (a.k.a. crater dating) on different basalt units in the Mare Insularum, and the results revealed that the lava flow units have a range of model ages from Imbrian to Eratosthenian (1.9 to 3.6 Ga). Subsequent studies found that the flooding may have occurred as early as 3.8 Ga (Zhao ZX et al., 2023), thus covering an extended time span.

3.3 Mare Nubium

The Mare Nubium (center location: 17.3°W, 20.6°S) is located in the ~750 km pre-Nectarian-aged Nubium basin (Wilhelms and McCauley, 1971; Figure 4a). Spectral data revealed composition differences among the basalts, with the TiO_2 abundance varying from 1% to 8% (Sato et al., 2017; Figure 4b). Crater dating showed that lava floodings within the Nubium basin have model ages ranging from Imbrian to Eratosthenian (2.8 to 3.7 Ga), with most being formed in the late Imbrian at 3.4–3.6 Ga (Hiesinger et al., 2011).

3.4 Typical Landforms

In the circum-Lalande region, multiple landforms are closely related to crater formation and basalt evolution, including ejecta rays, wrinkle ridges (WRs), and ring-moat dome structures

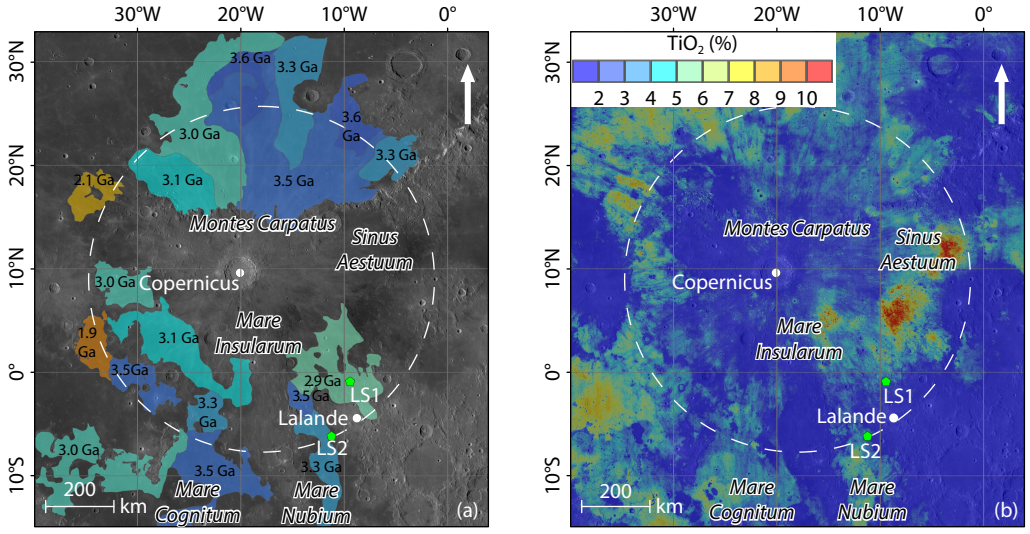

Figure 3. Context of the Mare Insularum. (a) Model ages of mare units (Hiesinger et al., 2011) overlaid on a WAC mosaic (Speyerer et al., 2011); (b) TiO_2 abundance map (Sato et al., 2017). The dashed white line portrays the approximate extent of the 1000-km Insularum basin. LS1 and LS2 are the candidate landing sites proposed for future crewed missions (see Section 4.1).

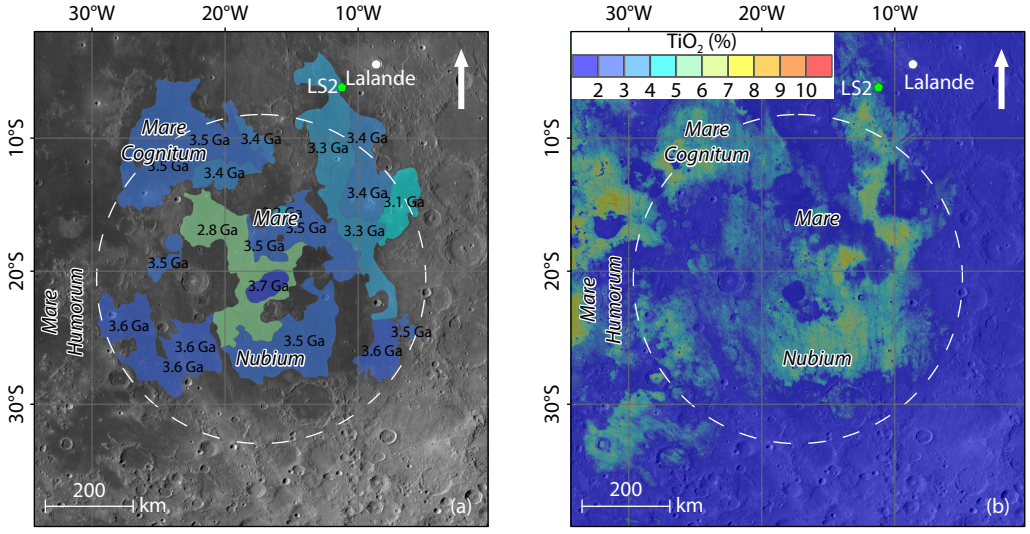

Figure 4. Context of the Mare Nubium. (a) Model ages of mare units (Hiesinger et al., 2011) overlaid on a WAC mosaic (Speyerer et al., 2011); (b) TiO_2 abundance map (Sato et al., 2017). The dashed white line portrays the approximate extent of the 750 km Nubium basin. LS2 is one of the candidate landing sites proposed for future crewed missions (see Section 4.1).

(RMDSs). Ejecta rays from Lalande and Copernicus are the most prominent features in this region (Figure 3). These optically immature Copernican-aged craters were formed during the most recent geological period in the lunar timescale. They provide critical information to help explain the impact flux during the Copernican epoch (Ravi et al., 2016), and their morphologies are vital for studying crater degradation and lunar regolith formation.

Wrinkle ridges (WRs) are widely distributed in the Mare Insularum and Nubium (Figures 2a and 5a). These ridges are the largest and most morphologically complex contractional landforms that occur exclusively in mare basalts (Watters, 2022). Because wrinkle ridges typically occur both radial to and concentric with the mare basin centers (Watters, 1988), they are thought to result from the subsidence and flexure of the lunar lithosphere, which was caused by the loading of mare basalts (i.e., tectonic compression; Watters, 1988, 2022). Wrinkle ridges could thus be considered paleo-stress indicators of the compressional history and thermal evolution of the shallow part of the lunar crust.

Ring-moat dome structures (RMDSs) are observed in this region from high-resolution NAC images (Figures 2a and 5b). These dome structures are small, circular mounds, typically ~200 m in diameter and ~3–4 m in height, that are surrounded by narrow and shallow moats (Zhang F et al., 2021). They are extensively developed in clusters in the Imbrian-aged mare basalts and have compositions similar to those of their host basalts (Zhang F et al., 2021). Currently, the remotely sensed images or products suggest two controversial origins for the RMDSs: (1) they occurred almost contemporaneously after the solidification of the host Imbrian-aged lava flows; (2) they formed as recently as in the Copernican epoch (Zhang F et al., 2021).

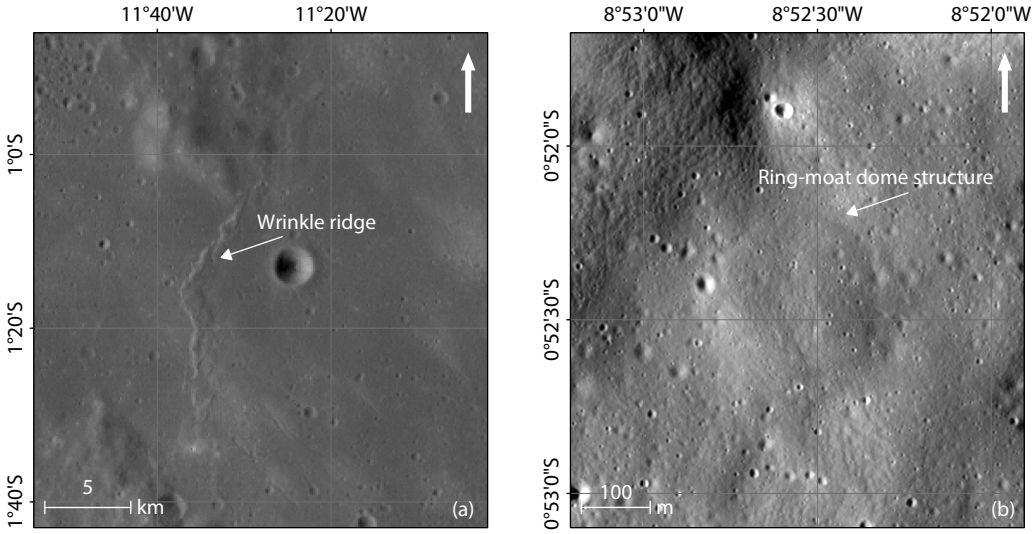

Figure 5. Example of typical landforms in the circum-Lalande region in the Mare Insularum. (a) WAC image (Speyerer et al., 2011) of a wrinkle ridge; (b) NAC image (Robinson et al., 2010) of a ring-moat dome structure.

4. Candidate Landing Sites and Recommended EVAs

4.1 Candidate Landing Sites

The priority of the crewed missions proposed in this study is to collect the speculated urKREEP samples to assess the LMO hypothesis. Because Th is considered a critical marker of KREEP, potential landing sites should be as close as possible to the Th-rich Lalande ejecta. To select suitable candidate landing sites for the crewed missions, the engineering constraints are similar to those of previous missions in terms of surface slopes (<10%), rock abundance (RA), illumination conditions, and real-time Earth–Moon direct communication (e.g., Ivanov et al., 2018). The flat basalt units in the Mare Insularum and Mare Nubium, which are partially covered by the Lalande and Copernicus ejecta (Figure 2a), are thus the best choice for a safe landing with respect to the engineering constraints. Two candidate landing sites, located respectively northwest and southeast of Lalande crater (Figure 2a), are proposed in this study. The proposed landing site 1 (LS1; location: 9.5°W, 0.9°S; Th: ~9.8 ppm) and landing site 2 (LS2; location: 11.1°W, 6.2°S; Th: ~10.1 ppm) are situated on the Th- and silica-rich Lalande ejecta in the Mare Insularum and Mare Nubium (Figures 2 and 6), respectively. In addition, these two sites are not far from the typical landforms in the circum-Lalande region (Figure 6), namely, the WRs and RMDSs. If the astronauts have the ability to traverse 10 km or more with the help of a lunar roving vehicle, it would be possible for them to collect samples from these typical landforms for a detailed analysis in the laboratory to unveil their ages, compositions, and evolution.

Detailed statistics on the topography, RA, and compositions at the proposed candidate landing sites and surrounding 5 km are presented in Table 2 and illustrated in Figure S1. The elevations at LS1 and LS2 are −1092 m and −1397 m, respectively. The slopes at the two sites are 1° and 1.8°, respectively, and the RAs are 0.3% and 0.5%, respectively. The mean slopes and RAs within 5 km of the two proposed landing sites are 2° and ≤0.5%, respectively. The

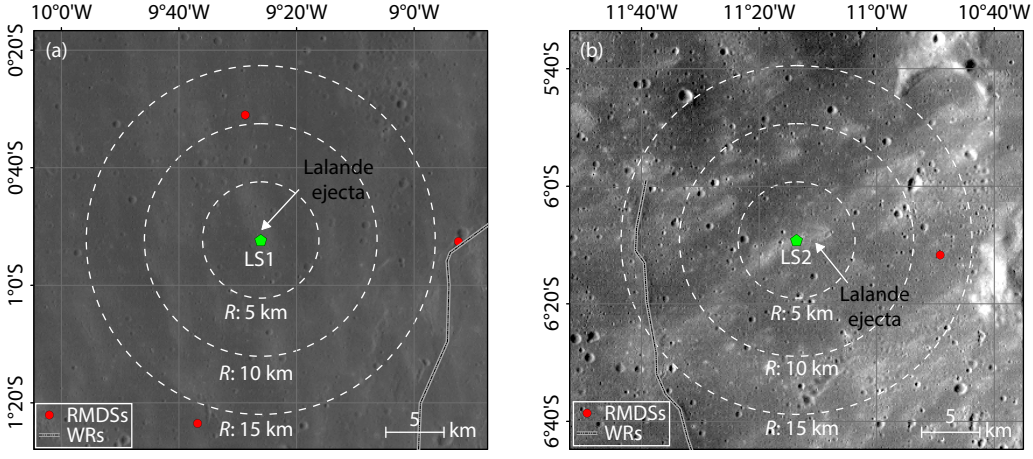

Figure 6. WAC image (Speyerer et al., 2011) of the proposed LS1 and LS2, which are situated on the Th- and silica-rich Lalande ejecta in the Mare Insularum and Mare Nubium, respectively. The wrinkle ridges (WRs) were identified by Thompson et al. (2017), and the ring-moat dome structures (RMDSs) were identified from NAC images (Robinson et al., 2010) in this study.

Table 2. Statistics on the topography, RA, and compositions at the proposed landing sites and surrounding 5 km.[a]

Area	Type	Min	Max	Mean	Stdev	Q1	Q2	Q3	LS
5 km around LS1	Elev. (m)	−1147	−1067	−1091	7	−1097	−1092	−1087	−1092
	Slope (°)	0	18.3	2	1.6	0.9	1.6	2.5	1
	RA (%)	0	7.8	0.4	0.4	0.2	0.3	0.4	0.3
	TiO_2 (wt%)	1	4.8	3	0.8	2.6	3.1	3.5	2.1
	FeO (wt%)	11.6	18.2	15.2	0.7	14.8	15.3	15.7	14.1
	Mg number	45.1	67.1	55.8	3.3	53.7	55.1	56.6	62.8
	CPX (wt%)	0	52	26.1	5.9	21.4	26.7	28.8	31.8
	OPX (wt%)	9.6	44.4	25.1	4.1	22.1	25.8	27.8	21.2
	OLV (wt%)	0	30.6	4.1	3.2	0	5.3	5.5	0
	PLG (wt%)	23	60	44.7	3.1	42.8	44.8	45.9	47
	Th (ppm)	9.8	9.8	9.8	9.8	9.8	9.8	9.8	9.8
	CF (μm)	8.21	8.33	8.27	0.02	8.24	8.26	8.28	8.24
5 km around LS2	Elev. (m)	−1468	−1380	−1403	10	−1410	−1401	−1396	−1397
	Slope (°)	0	18.1	2	1.7	0.9	1.6	2.3	1.8
	RA (%)	0	5.2	0.5	0.4	0.3	0.4	0.5	0.5
	TiO_2 (wt%)	1	5.3	3.4	0.8	2.9	3.5	3.9	3.6
	FeO (wt%)	11.6	16.9	15.4	0.7	15	15.4	15.7	13.7
	Mg number	40.8	64.7	50.9	2.5	49.5	51.2	52.2	56.6
	CPX (wt%)	9.2	45.5	24.6	4.8	20.6	25.3	27.3	28.8
	OPX (wt%)	0	32.4	19.1	3.8	15.8	20.2	21.5	14.4
	OLV (wt%)	0	22.8	9.2	2.8	5.5	10.1	10.6	4.8
	PLG (wt%)	27	61	47.2	2.9	44.8	46.8	48.8	52
	Th (ppm)	10.1	10.1	10.1	10.1	10.1	10.1	10.1	10.1
	CF (μm)	8.05	8.37	8.26	0.03	8.25	8.27	8.29	8.24

[a]Q1, Q2, and Q3 indicate quartiles. CPX, clinopyroxene; OPX, orthopyroxene; OLV, olivine; PLG, plagioclase. LS, landing site.

flat surface and the low rock abundance suggest that the proposed sites would be suitable for a safe landing. In addition, the geolocation at the low latitude on the lunar nearside indicates they would fully meet the needs of real-time Earth–Moon communication.

Although a relatively noticeable difference exists in the TiO_2 abundance between LS1 and LS2 (2.1 wt% vs. 3.6 wt%), the average abundances within 5 km of the two sites are essentially consistent (3 wt% vs. 3.4 wt%), indicating the basalts are low-Ti basalts (Giguere et al., 2000). On the contrary, the FeO abundances at the two sites are relatively consistent, either in the surrounding area (15.2 wt% vs. 15.4 wt%) or at the landing site (14.1 wt% vs. 13.7 wt%).

The average abundance of olivine is the lowest, whereas plagioclase is the most abundant in the vicinities of both sites, accounting for ~50% of the total mass. The average abundance of clinopyroxene is basically equal to that of orthopyroxene within 5 km of LS1 (26.1 wt% vs. 25.1 wt%). However, the abundance of clinopyroxene is slightly higher than that of orthopyroxene in the surroundings of LS2 (24.6 wt% vs. 19.1 wt%). The mare basalts are products of partial melting of the lunar mantle, and the Mg number values at the two landing sites (62.8 vs. 56.6) suggest the magma have undergone a moderate evolution. Although the two proposed sites are not far away (~170 km), they are geographically separated by the highlands (Figure 2a). The difference in mineral composition indicates that the mantle sources of the two mare basalts have different chemical properties and that the basalt samples are appropriate agents for studying the lunar thermal evolution.

4.2 Proposed EVAs for the Astronauts

4.2.1 Collecting KREEP-rich samples

The KREEP components are thought to have elevated concentrations of K, REEs, P, Th, U, and other trace elements. It may be difficult to distinguish KREEP-rich materials from mare basalts and other non-mare ejecta by the naked eye. To address such a situation, the candidate landing sites proposed in this study are situated on the Lalande ejecta (Figure 6), which is rich in Th (a marker for KREEP). In addition, we recommend that the astronauts be equipped with a miniaturized intelligent geochemical instrument (e.g., a portable gamma-ray detector), which would be capable of the real-time identification of KREEP-rich materials. The implementation of these measures would maximize the likelihood of

collecting KREEP-rich samples at the candidate landing sites during EVAs.

4.2.2 Screening clast samples

Experience gained from analyzing the returned lunar regolith samples demonstrated that modern instruments are capable of accurately analyzing substances as small as tens of microns, a finding that has great scientific implications. For example, three glass beads in the Chang'e-5 samples suggested volcanoes were erupting on the Moon while dinosaurs roamed Earth just 120 million years ago (Wang BW et al., 2024). Given that the total weight of the returned samples is usually limited by engineering conditions, scientists routinely expect the astronauts to selectively collect high-value samples to maximize the research output. When the geological age of the landing area is old, in addition to local bedrock debris, the lunar regolith often contains a variety of exotic materials. Therefore, astronauts are expected to perform screening to collect millimeter-sized clast samples. A large quantity of exotic clasts from other geological units on the Moon could thus be collected by removing oversized or undersized materials. These exotic materials would be of great significance for studying the formation and evolution of the Moon. Specific to the landing area proposed in this paper, collection refers to the acquisition of KREEP- and silica-rich Lalande ejecta, Copernicus ejecta, underlying basalts, breccias, and other exotic materials.

4.2.3 Drilling regolith cores

The formation of a crater would involve ejection of materials and their deposition in distal places. According to the empirical equation proposed by Sharpton (2014; see Supplementary Text 1), the equivalent thickness of ejecta from the 400-Ma Lalande (Xu LY et al., 2022) and 800-Ma Copernicus (Bogard et al., 1994) craters at the proposed landing sites are dozens of centimeters thick, respectively (Figures 7 and S2). Because Copernicus is older than Lalande, its ejecta should be covered by Th-rich Lalande ejecta when they deposited at the proposed landing sites (Figure 7a). Both Copernicus and Lalande were formed on the lunar highlands, their anorthositic ejecta and the underlying mare basalts have different lithologies. The continual impact and gardening processes that form the regolith would gradually have mixed these three distinct materials (Figure 7b). However, the structure and formation mechanism of lunar regolith are still not well understood. If the astronauts drilled regolith cores in places blanketed by Copernicus ejecta, Lalande ejecta, or both (Figure 7c), the cores would be critical for understanding the downward and upward migration phenomena of the materials and deciphering the lunar bombardment history since the Copernican epoch.

5. Problems Related to Samples from the Circum-Lalande Region

From implementation of the suggested EVAs, we would expect a wide variety of samples, such as Th- and silica-rich Lalande ejecta, Copernicus ejecta, mare basalts, and regolith cores, to be collected in the vicinity of the two candidate landing sites. Analysis of these samples in laboratories with modern equipment would shed light on many critical scientific issues. The following sections discuss some problems that could be addressed by examination of the samples returned from the proposed landing sites.

5.1 Exploration of the Speculated urKREEP

Theoretically, KREEP components are believed to be the last products in the final stage of the LMO evolution, and urKREEP may have crystallized from the primordial residual liquid (e.g., see Warren and Wasson, 1979; Warren, 1985). The crystallization of urKREEP indicates the final solidification of the LMO; thus, it retains key records of the scale, differentiation, and duration of the LMO. The KREEP-rich materials (i.e., derivatives of urKREEP, such as KREEP-rich basalts and breccias) have been found in lunar samples and meteorites (e.g., see Meyer et al., 1971; Gnos et al., 2004). Two petrogenetic models have been proposed for the KREEP materials (Warren and Wasson, 1979): (1) dilution of urKREEP with crustal or mantle materials during assimilation, or

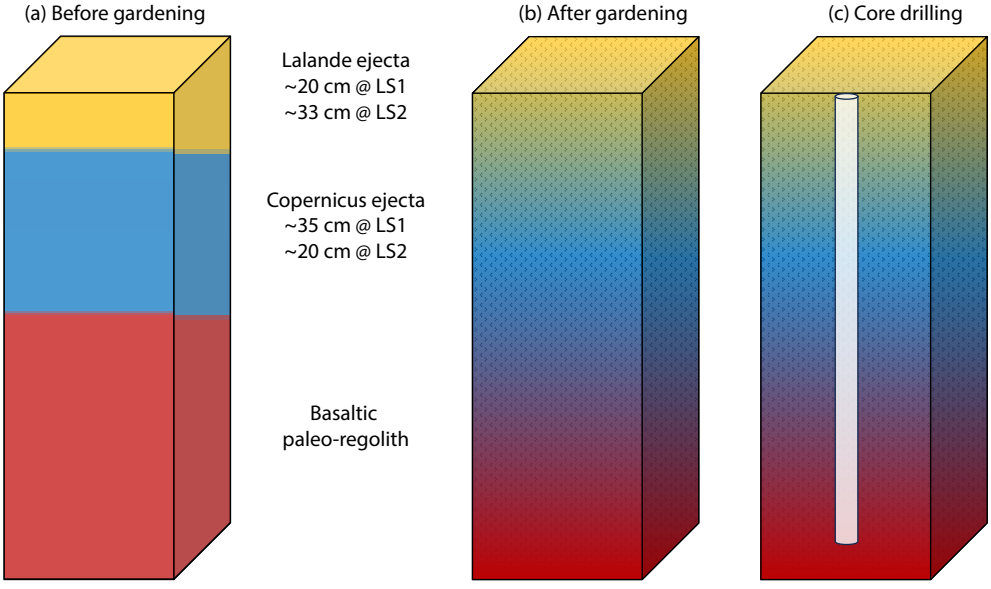

Figure 7. Schematic diagram of drilling regolith cores on the ejecta blanket.

zone refining (endogenous pristine basalts); (2) impact-induced brecciation, or homogenization of KREEP-bearing lithologies (impact breccias or melts). However, urKREEP that crystallized directly from the residual magma has not yet been found.

Because of the lack of samples, the existence of urKREEP is doubted and its formation time cannot be dated directly. Analysis of isotopic systems in the pristine samples, whose genesis may be related to the urKREEP (e.g., KREEP-rich basalts and Mg suites), has provided constraints on the formation time of urKREEP. For example, Rb–Sr model ages of breccias imply that crystallization of the LMO was essentially complete at 4.4–4.5 Ga (Warren and Wasson, 1979); Sm–Nd model ages of four "high-Mg" highland rocks indicate that a large-scale differentiation event had climaxed at ~4.33 ± 0.08 Ga (Carlson and Lugmair, 1981); and the Lu–Hf model ages of KREEP-rich samples suggest that the formation of KREEP and crystallization of the LMO occurred around 4.35–4.43 Ga (Sprung et al., 2013). Returned Th-rich samples would thus be of great significance for exploring the existence and formation of urKREEP, determining the solidification time of the LMO, and clarifying the HPEs–KREEP coupling hypothesis.

5.2 Investigation of the Relationship Between HPEs and Volcanism

Crater dating on different mare basalt units, radiometric dating on samples returned by the Apollo, Luna, and Chang'e-5/6 missions, as well as lunar meteorites, reveal that the volcanism on the lunar surface have lasted ~3 Ga, beginning at ~4.35 Ga and ceasing at ~1.2 Ga (Nyquist and Shih, 1992; Fernandes and Burgess, 2005; Terada et al., 2007; Hiesinger et al., 2011; Joy and Arai, 2013; Pasckert et al., 2015; Snape et al., 2019; Li QL et al., 2021; Zhang QWL et al., 2024). The ages of the mare basalts suggest that two surges of volcanic activity occurred on the Moon: a first peak at 3.2–3.8 Ga and a second at ~2 Ga (Kato et al., 2017). The Chang'e-5 samples even indicated volcanic eruptions on the Moon at ~120 Ma (Wang BW et al., 2024).

The PKT (Jolliff et al., 2000) hosts the majority of mare basalts on the lunar surface (Nelson et al., 2014). It is also an area enriched in HPEs, most notably Th, U, and K (Lawrence et al., 1998; Figure 1). Enrichment of the HPEs has been proposed to be responsible for the flooding of mare basalts (Ogawa, 2018), such as the 2.9-Ga KREEP magmatism (Borg et al., 2004). However, the relationship between HPEs and lunar volcanism is rather complex and unclear. For example, the Chang'e-5 samples indicated that the mantle source for the 2-Ga mare volcanism was KREEP free (Tian HC et al., 2021). The Chang'e-6 samples revealed that two episodes of basaltic volcanism had occurred in the farside; the 4.2-Ga eruption had a KREEP-rich mantle source, and the source of the 2.8-Ga flooding was KREEP poor (Zhang QWL et al., 2024). At present, the distribution of HPEs in the lunar mantle is still poorly understood. For example, reasons for the shift of a source depleted in HPEs observed in the Chang'e-6 samples are unclear. The volcanic activities in the Mare Insularum and Mare Nubium are long-lasting (Hiesinger et al., 2011; Zhao ZX et al., 2023), and the compositions of the basalts are diverse. Therefore, basalt samples returned from the proposed landing sites would contribute to studying the relationship between the HPEs and volcanism, as well as to the thermal evolution of the lunar mantle.

5.3 Refinement of the Lunar Chronology Function

The lunar chronology function is critical for determining the model ages of unsampled geological units on the Moon. It links the radiometric ages of returned samples and the crater size–frequency distribution of the crater counting unit (e.g., see Neukum, 1984; Yue ZY et al., 2022; Hiesinger et al., 2023; Werner et al., 2023). The formation age of the Copernicus crater is used as an important anchor point when defining the lunar chronology function (e.g., see Neukum, 1984). However, the impact that formed the Copernicus crater is only indirectly, and accordingly poorly constrained. In fact, among all the samples returned by the Apollo missions, only two samples (12032/12033) were considered to have originated from the Copernicus crater (Hubbard et al., 1971). The present dilemma is that the radiometric dating results from different techniques are not consistent (Silver, 1971; Eberhardt et al., 1973; Alexander et al., 1977; Bogard et al., 1994; Barra et al., 2006). In addition, on the basis of the good agreement among the high-Th content, crater ages, and Fe–Ti concentrations of regolith in the Lalande area, Gnos et al. (2004) proposed the Copernican-aged Lalande crater as the most plausible source region for the lunar meteorite SaU 169. However, Xu LY et al. (2022) found that the model age of Lalande crater (~410 Ma) was inconsistent with any of the radio-isotopic ages (3909 Ma, ~2800 Ma, ~200 Ma, <0.34 Ma) recorded in the SaU 169 (Gnos et al., 2004). They thus argued that the Lalande is unlikely to be the source crater.

Ray materials from the 800-Ma Copernicus (Bogard et al., 1994) and 410-Ma Lalande crater (Xu LY et al., 2022) can be clearly observed when viewing from the LROC WAC mosaic (Figure 2a). The proposed landing sites are situated on the ejecta; therefore, definitive samples from Copernicus and/or Lalande craters could easily be collected. In addition, we would expect samples of mare basalts that erupted at different times (e.g., 2.9 Ga at LS1 and 3.3 Ga at LS2) to be collected (Figure 3). Conducting radiometric dating on all these samples would not only validate existing claims regarding the ages of Copernicus and Lalande craters, but could also provide additional anchor points for the refinement of lunar cratering chronology.

5.4 Investigation of Volatiles in the Regolith

According to the giant impact theory, scientists initially believed that the Moon was extremely depleted in volatiles. However, ongoing studies have revealed that the lunar regolith contains various volatile components (e.g., hydrogen/hydroxyl/water, chorine, sulfur). The main sources of volatiles in the regolith are the solar wind, small bodies in the solar system (i.e., comets and meteorites), and the lunar interior (Ivanov, 2014). They are fundamental tracers of the Moon's origin, evolution, and interaction with its space environment (Hayne, 2018). Therefore, lunar volatiles have both scientific and exploration significance (Pieters et al., 2009; Hurley et al., 2017). For scientific research, the volatiles hold crucial clues about the sources and history of volatiles in the inner solar system. For example, the water content in the mantle source for the Chang'e-5 basalt is estimated to be as low as 1–5 ppm, indicating that the volcanism was not driven by abundant

water (Hu S et al., 2021). For exploration, the hydrogen/hydroxyl/water represents a critical resource that could be mined for propellant production and life support (i.e., *in situ* resource utilization; Hurley et al., 2017). Therefore, investigation of the lunar volatiles has become a hot area in recent lunar missions. For example, one of the major objectives of the Chang'e-7 mission is to investigate the distribution and origin of water ice and volatile components at the lunar south pole (Wang C et al., 2024).

Our understanding of lunar volatiles has progressed substantially in the past decades. Because the distribution and abundance of lunar volatiles are affected both by geological activity and the space environment, many questions still need to be answered by comprehensively evaluating lunar samples from different regions. The collection of intact drilled basaltic regolith cores, together with the Apollo, Luna, and Chang'e samples, would fuel an in-depth study of the following issues: (1) inventories and sources of the internal volatiles since the formation of the Moon; (2) inventories and fluxes of exogenous volatiles over billions of years; (3) spatial and temporal distribution of exogenous and internal volatiles; and (4) migration of the volatiles in the lunar regolith.

6. Conclusions

The primordial KREEP (i.e., urKREEP) suggested by the LMO hypothesis has not been found in previous lunar samples or meteorites. Because the risks of crewed missions have decreased substantially with the advancement of technology, two candidate landing sites in the circum-Lalande region, which are enriched in Th (an indicator of KREEP), are proposed for future lunar crewed missions, with the aim of searching for the speculated urKREEP. From the perspective of engineering constraints, both sites are safe in terms of surface slope, rock abundance, illumination condition, and Earth–Moon direct communication. Extravehicular activities, such as collecting KREEP-rich materials, screening clast samples, and drilling regolith cores, can be envisioned. With the collection of a wide variety of samples, such as Th-rich Lalande ejecta, basalts, Copernicus ejecta, and regolith cores, the returned samples would be valuable for exploring the speculated urKREEP, revealing the relationship between HPEs and volcanism, refining the lunar chronology function, and investigating volatiles in the regolith.

Acknowledgments

The authors thank the three anonymous reviewers for their constructive and insightful reviews, which substantially improved the quality of the manuscript. We also appreciate SuFang Hu and HeJiu Hui for effective editorial handling. This research was supported by the National Key Research and Development Program of China (Grant No. 2022YFF0503104), the National Natural Science Foundation of China (Grant Nos. 42241111, 62227901, and 42441826), the Macao Young Scholars Program (Grant No. AM201902), and the Key Research Program of the Institute of Geology and Geophysics, Chinese Academy of Sciences (Grant No. IGGCAS-202401).

References

Alexander, E. C., Jr., Coscio, M. R., Jr., Dragon, J. C., Pepin, R. O., and Saito, K. (1977). K/Ar dating of lunar soils III: Comparison of ^{39}Ar-^{40}Ar and conventional techniques: 12032 and the age of Copernicus. In *Proceedings of the 8th Lunar Science Conference* (pp. 2725–2740). Houston, Texas, USA: Pergamon Press.

Barker, M. K., Mazarico, E., Neumann, G. A., Zuber, M. T., Haruyama, J., and Smith, D. E. (2016). A new lunar digital elevation model from the Lunar Orbiter Laser Altimeter and SELENE Terrain Camera. *Icarus*, *273*, 346–355. https://doi.org/10.1016/j.icarus.2015.07.039

Barra, F., Swindle, T. D., Korotev, R. L., Jolliff, B. L., Zeigler, R. A., and Olson, E. (2006). ^{40}Ar/^{39}Ar dating of Apollo 12 regolith: Implications for the age of Copernicus and the source of nonmare materials. *Geochim. Cosmochim. Acta*, *70*(24), 6016–6031. https://doi.org/10.1016/j.gca.2006.09.013

Bogard, D. D., Garrison, D. H., Shih, C. Y., and Nyquist, L. E. (1994). ^{39}Ar-^{40}Ar dating of two lunar granites: The age of Copernicus. *Geochim. Cosmochim. Acta*, *58*(14), 3093–3100. https://doi.org/10.1016/0016-7037(94)90181-3

Borg, L. E., Shearer, C. K., Asmerom, Y., and Papike, J. J. (2004). Prolonged KREEP magmatism on the Moon indicated by the youngest dated lunar igneous rock. *Nature*, *432*(7014), 209–211. https://doi.org/10.1038/nature03070

Carlson, R. W., and Lugmair, G. W. (1981). Sm-Nd age of Iherzolite 67667: Implications for the processes involved in lunar crustal formation. *Earth Planet. Sci. Lett.*, *56*, 1–8. https://doi.org/10.1016/0012-821X(81)90112-6

Cifani, G., Darrau, A., Rometsch, F. A. A. S. D. T., Alvarez, G., Duvet, L., and Biesbroek, R. (2024). Argonaut: ESA's versatile lunar lander enabling multiple moon missions. In *Proceedings of the IAF Human Spaceflight Symposium* (p. 88203). Milan, Italy: IAF.

Cui, Z. X., Yang, Q., Zhang, Y. Q., Wang, C. Y., Xian, H. Y., Chen, Z. M., Xiao, Z. Y., Qian, Y. Q., Head, J. W., III, … Xu, Y. G. (2024). A sample of the Moon's far side retrieved by Chang'e-6 contains 2.83-billion-year-old basalt. *Science*, *386*(6728), 1395–1399. https://doi.org/10.1126/science.adt1093

Eberhardt, P., Geiss, J., Grögler, N., and Stettler, A. (1973). How old is the crater Copernicus?. *Moon*, *8*(1), 104–114. https://doi.org/10.1007/BF00562752

Fernandes, V. A., and Burgess, R. (2005). Volcanism in Mare Fecunditatis and Mare Crisium: Ar-Ar age studies. *Geochim. Cosmochim. Acta*, *69*(20), 4919–4934. https://doi.org/10.1016/j.gca.2005.05.017

Giguere, T. A., Taylor, G. J., Hawke, B. R., and Lucey, P. G. (2000). The titanium contents of lunar mare basalts. *Meteorit. Planet. Sci.*, *35*(1), 193–200. https://doi.org/10.1111/j.1945-5100.2000.tb01985.x

Gnos, E., Hofmann, B. A., Al-Kathiri, A., Lorenzetti, S., Eugster, O., Whitehouse, M. J., Villa, I. M., Jull, A. J. T., Eikenberg, J., … Greenwood, R. C. (2004). Pinpointing the source of a lunar meteorite: Implications for the evolution of the moon. *Science*, *305*(5684), 657–659. https://doi.org/10.1126/science.1099397

Greenhagen, B. T., Lucey, P. G., Wyatt, M. B., Glotch, T. D., Allen, C. C., Arnold, J. A., Bandfield, J. L., Bowles, N. E., Hanna, K. L. D., … Paige, D. A. (2010). Global silicate mineralogy of the moon from the diviner lunar radiometer. *Science*, *329*(5998), 1507–1509. https://doi.org/10.1126/science.1192196

Haskin, L. A., Gillis, J. J., Korotev, R. L., and Jolliff, B. L. (2000). The materials of the lunar Procellarum KREEP Terrane: A synthesis of data from geomorphological mapping, remote sensing, and sample analyses. *J. Geophys. Res.: Planets*, *105*(E8), 20403–20415. https://doi.org/10.1029/1999JE001128

Hayne, P. O. (2018). Lunar polar volatiles: Current understanding, recent discoveries, and future exploration. In *Proceedings of the Lunar Polar Volatiles 2018* (p. 5017). Laurel, Maryland, USA: LPI.

Hiesinger, H., Head, J. W., III, Wolf, U., Jaumann, R., and Neukum, G. (2011). Ages and stratigraphy of lunar mare basalts: A synthesis. In W. A. Ambrose, et al. (Eds.), *Recent Advances and Current Research Issues in Lunar Stratigraphy* (pp. 1–51). Boulder, Colorado, USA: The Geological Society of America. https://doi.org/10.1130/2011.2477(01)

Hiesinger, H., van der Bogert, C. H., Michael, G., Schmedemann, N., Iqbal, W., Robbins, S. J., Ivanov, B., Williams, J. P., Zanetti, M., … Head, J. W., III (2023). The lunar cratering chronology. *Rev. Mineral. Geochem.*, *89*(1), 401–451. https://doi.org/10.2138/rmg.2023.89.10

Hu, S., He, H. C., Ji, J. L., Lin, Y. T., Hui, H. J., Anand, M., Tartèse, R., Yan, Y. H., Hao, J. L., Li, R. Y., … Ouyang, Z. Y. (2021). A dry lunar mantle reservoir for young

mare basalts of Chang'e-5. *Nature, 600*(7887), 49–53. https://doi.org/10.1038/s41586-021-04107-9

Hubbard, N. J., Meyer, C., Gast, P. W., and Wiesmann, H. (1971). The composition and derivation of Apollo 12 soils. *Earth Planet. Sci. Lett.*, *10*(3), 341–350. https://doi.org/10.1016/0012-821X(71)90040-9

Hurley, D. M., and LEAG Executive Committee (2017). Lunar volatiles as a resource for science and exploration. In *Proceedings of the Planetary Science Vision 2050 Workshop* (p. 8096). Washington, DC, USA: LPI.

Ivanov, A. V. (2014). Volatiles in lunar regolith samples: A survey. *Sol. Syst. Res.*, *48*(2), 113–129. https://doi.org/10.1134/S0038094614020038

Ivanov, M. A., Abdrakhimov, A. M., Basilevsky, A. T., Demidov, N. E., Guseva, E. N., Head, J. W., Hiesinger, H., Kohanov, A. A., and Krasilnikov, S. S. (2018). Geological characterization of the three high-priority landing sites for the Luna-Glob mission. *Planet. Space Sci.*, *162*, 190–206. https://doi.org/10.1016/j.pss.2017.08.004

Jolliff, B. L., Gillis, J. J., Haskin, L. A., Korotev, R. L., and Wieczorek, M. A. (2000). Major lunar crustal terranes: Surface expressions and crust–mantle origins. *J. Geophys. Res.: Planets*, *105*(E2), 4197–4216. https://doi.org/10.1029/1999je001103

Joy, K. H., and Arai, T. (2013). Lunar meteorites: New insights into the geological history of the Moon. *Astron. Geophys.*, *54*(4), 4.28–4.32. https://doi.org/10.1093/astrogeo/att121

Kato, S., Morota, T., Yamaguchi, Y., Watanabe, S. I., Otake, H., and Ohtake, M. (2017). Magma source transition of lunar mare volcanism at 2.3 Ga. *Meteorit. Planet. Sci.*, *52*(9), 1899–1915. https://doi.org/10.1111/maps.12896

Lawrence, D. J., Feldman, W. C., Barraclough, B. L., Binder, A. B., Elphic, R. C., Maurice, S., and Thomsen, D. R. (1998). Global elemental maps of the moon: The lunar prospector gamma-ray spectrometer. *Science*, *281*(5382), 1484–1489. https://doi.org/10.1126/science.281.5382.1484

Lemelin, M., Lucey, P. G., Gaddis, L. R., Hare, T., and Ohtake, M. (2016). Global map products from the Kaguya Multiband Imager at 512 ppd: Minerals, FeO, and OMAT. In *Proceedings of the 47th Lunar and Planetary Science Conference* (p. 2994). The Woodlands, Texas, USA: LPI.

Levin, J. N., Evans, A. J., Andrews-Hanna, J. C., and Daubar, I. J. (2025). Lunar crustal KREEP distribution. *J. Geophys. Res.: Planets*, *130*(1), e2024JE008418. https://doi.org/10.1029/2024JE008418

Li, B., Ling, Z. C., Zhang, J., Chen, J., Liu, C. Q., and Bi, X. Y. (2018). Geological mapping of lunar highland crater Lalande: Topographic configuration, morphology and cratering process. *Planet. Space Sci.*, *151*, 85–96. https://doi.org/10.1016/j.pss.2017.11.007

Li, C. L., Hu, H., Yang, M. F., Liu, J. J., Zhou, Q., Ren, X., Liu, B., Liu, D. W., Zeng, X. G., … Ouyang, Z. Y. (2024). Nature of the lunar far-side samples returned by the Chang'E-6 mission. *Natl. Sci. Rev.*, *11*(11), nwae328. https://doi.org/10.1093/nsr/nwae328

Li, Q. L., Zhou, Q., Liu, Y., Xiao, Z. Y., Lin, Y. T., Li, J. H., Ma, H. X., Tang, G. Q., Guo, S., ... Li, X. H. (2021). Two-billion-year-old volcanism on the Moon from Chang'e-5 basalts. *Nature*, *600*(7887), 54–58. https://doi.org/10.1038/s41586-021-04100-2

Lin, Y., Shen, W., Liu, Y., Xu, L., Hofmann, B. A., Mao, Q., Tang, G. Q., Wu, F., and Li, X. H. (2012). Very high-K KREEP-rich clasts in the impact melt breccia of the lunar meteorite SaU 169: New constraints on the last residue of the Lunar Magma Ocean. *Geochim. Cosmochim. Acta*, *85*, 19–40. https://doi.org/10.1016/j.gca.2012.02.011

Liu, D. Y., Jolliff, B. L., Zeigler, R. A., Korotev, R. L., Wan, Y. S., Xie, H. Q., Zhang, Y. H., Dong, C. Y., and Wang, W. (2012). Comparative zircon U–Pb geochronology of impact melt breccias from Apollo 12 and lunar meteorite SaU 169, and implications for the age of the Imbrium impact. *Earth Planet. Sci. Lett., 319–320*, 277–286. https://doi.org/10.1016/j.epsl.2011.12.014

Melosh, H. J. (1989). *Impact Cratering: A Geologic Process*. New York, USA: Oxford University Press.

Meyer, C. Jr., Brett, R., Hubbard, N. J., Morrison, D. A., McKay, D. S., Aitken, F. K., Takeda, H., and Schonfeld, E. (1971). Mineralogy, chemistry, and origin of the KREEP component in soil samples from the Ocean of Storms. In *Proceedings of the 2nd Lunar Science Conference* (pp. 393–411). New York, USA: Pergamon Press.

Mitrofanov, I. G., Tretyakov, V. I., and Zelenyi, L. M. (2021). Mission of Luna-25, as the first step of Russian robotic moon exploration program. In *Proceedings of the 52nd Lunar and Planetary Science Conference* (p. 2032). The Woodlands, Texas, USA: LPI

Moriarty, D. P., III, Dygert, N., Valencia, S. N., Watkins, R. N., and Petro, N. E. (2021). The search for lunar mantle rocks exposed on the surface of the Moon. *Nat. Commun.*, *12*(1), 4659. https://doi.org/10.1038/s41467-021-24626-3

National Research Council. (2007). *The Scientific Context for Exploration of the Moon*. Washington, DC: National Academies Press. https://doi.org/10.17226/11954

Nelson, D. M., Koeber, S. D., Daud, K., Robinson, M. S., Watters, T. R., Banks, M. E., and Williams, N. R. (2014). Mapping lunar Maria extents and Lobate scarps using LROC image products. In *Proceedings of the 45th Lunar and Planetary Science Conference* (p. 2861). The Woodlands, Texas, USA: LPI.

Neukum, G. (1984). *Meteorite Bombardment and Dating of Planetary Surfaces*. Washington, DC, USA: NASA.

Niu, R., Zhang, G., Mu, L. L., Lin, Y. T., Liu, J. Z., Bo, Z., Dai, W., and Zhang, P. (2023). Scientific objectives and suggestions on landing site selection of manned lunar exploration engineering. *J. Astronaut. (in Chinese)*, *44*(9), 1280–1290. https://doi.org/10.3873/j.issn.1000-1328.2023.09.002

Nyquist, L. E., and Shih, C. Y. (1992). The isotopic record of lunar volcanism. *Geochim. Cosmochim. Acta*, *56*(6), 2213–2234. https://doi.org/10.1016/0016-7037(92)90185-L

Ogawa, M. (2018). The effects of magmatic redistribution of heat producing elements on the lunar mantle evolution inferred from numerical models that start from various initial states. *Planet. Space Sci.*, *151*, 43–55. https://doi.org/10.1016/j.pss.2017.10.015

Palanivel, V. (2024). New frontiers in lunar exploration: Chandrayaan-3 mission & beyond. In *Proceedings of the 75th International Astronautical Congress*. Milan, Italy: IAF.

Parmentier, E. M., Zhong, S., and Zuber, M. T. (2002). Gravitational differentiation due to initial chemical stratification: Origin of lunar asymmetry by the creep of dense KREEP?. *Earth Planet. Sci. Lett.*, *201*(3-4), 473–480. https://doi.org/10.1016/S0012-821X(02)00726-4

Pasckert, J. H., Hiesinger, H., and van der Bogert, C. H. (2015). Small-scale lunar farside volcanism. *Icarus*, *257*, 336–354. https://doi.org/10.1016/j.icarus.2015.04.040

Pieters, C. M., Goswami, J. N., Clark, R. N., Annadurai, M., Boardman, J., Buratti, B., Combe, J. P., Dyar, M. D., Green, R. O., … Varanasi, P. (2009). Character and spatial distribution of OH/H_2O on the surface of the moon seen by M^3 on Chandrayaan-1. *Science, 326*(5952), 568–572. https://doi.org/10.1126/science.1178658

Powell, T. M., Horvath, T., Robles, V. L., Williams, J. P., Hayne, P. O., Gallinger, C. L., Greenhagen, B. T., McDougall, D. S., and Paige, D. A. (2023). High-resolution nighttime temperature and rock abundance mapping of the moon using the diviner lunar radiometer experiment with a model for topographic removal. *J. Geophys. Res.: Planets*, *128*(2), e2022JE007532. https://doi.org/10.1029/2022JE007532

Ravi, S., Meyer, H. M., Mahanti, P., and Robinson, M. S. (2016). On the usefulness of optical maturity for relative age classification of fresh craters. In *Proceedings of the American Geophysical Union, Fall Meeting* (p. P53A-2166). San Francisco, California, USA: American Geophysical Union.

Robinson, M. S., Brylow, S. M., Tschimmel, M., Humm, D., Lawrence, S. J., Thomas, P. C., Denevi, B. W., Bowman-Cisneros, E., Zerr, J., … Hiesinger, H. (2010). Lunar reconnaissance orbiter camera (LROC) instrument overview. *Space Sci. Rev.*, *150*(1), 81–124. https://doi.org/10.1007/s11214-010-9634-2

Sato, H., Robinson, M. S., Lawrence, S. J., Denevi, B. W., Hapke, B., Jolliff, B. L., and Hiesinger, H. (2017). Lunar mare TiO_2 abundances estimated from UV/Vis reflectance. *Icarus*, *296*, 216–238. https://doi.org/10.1016/j.icarus.2017.06.013

Schultz, P. H., and Crawford, D. A. (2011). Origin of nearside structural and geochemical anomalies on the Moon. In W. A. Ambrose, et al. (Eds.), *Recent Advances and Current Research Issues in Lunar Stratigraphy* (pp. 141–159). Boulder, Colorado, USA: The Geological Society of America. https://doi.org/10.1130/2011.2477(07)

Sharpton, V. L. (2014). Outcrops on lunar crater rims: Implications for rim

construction mechanisms, ejecta volumes and excavation depths. *J. Geophys. Res.: Planets*, *119*(1), 154–168. https://doi.org/10.1002/2013JE004523

Silver, L. T. (1971). U-Th-Pb isotope systems in Apollo 11 and 12 regolithic materials and a possible age for the Copernican impact. In *Proceedings of the 52nd Annual Meeting of the American Geophysical Union* (p. 534). Washington, DC, USA: American Geophysical Union.

Smith, J. V., Anderson, A. T., Newton, R. C., Olsen, E. J., Crewe, A. V., Isaacson, M. S., Johnson, D., and Wyllie, P. J. (1970). Petrologic history of the moon inferred from petrography, mineralogy and petrogenesis of Apollo 11 rocks. In *Proceedings of the Apollo 11 Lunar Science Conference* (pp. 897–925). New York, USA: Pergamon Press.

Smith, M., Craig, D., Herrmann, N., Mahoney, E., Krezel, J., McIntyre, N., and Goodliff, K. (2020). The Artemis program: An overview of NASA's activities to return humans to the moon. In *Proceedings of 2020 IEEE Aerospace Conference* (pp. 1–10). Big Sky, Montana, USA: IEEE. https://doi.org/10.1109/AERO47225.2020.9172323

Snape, J. F., Nemchin, A. A., Whitehouse, M. J., Merle, R. E., Hopkinson, T., and Anand, M. (2019). The timing of basaltic volcanism at the Apollo landing sites. *Geochim. Cosmochim. Acta*, *266*, 29–53. https://doi.org/10.1016/j.gca.2019.07.042

Speyerer, E. J., Robinson, M. S., Denevi, B. W., and LROC Science Team (2011). Lunar reconnaissance orbiter camera global morphological map of the moon. In *Proceedings of the 42nd Lunar and Planetary Science Conference* (p. 2387). The Woodlands, Texas, USA: LPI.

Sprung, P., Kleine, T., and Scherer, E. E. (2013). Isotopic evidence for chondritic Lu/Hf and Sm/Nd of the Moon. *Earth Planet. Sci. Lett.*, *380*, 77–87. https://doi.org/10.1016/j.epsl.2013.08.018

Terada, K., Anand, M., Sokol, A. K., Bischoff, A., and Sano, Y. (2007). Cryptomare magmatism 4.35Gyr ago recorded in lunar meteorite Kalahari 009. *Nature, 450*(7171), 849–852. https://doi.org/10.1038/nature06356

Thompson, T. J., Robinson, M. S., Watters, T. R., and Johnson, M. B. (2017). Global lunar wrinkle ridge identification and analysis. In *Proceedings of the 48th Lunar and Planetary Science Conference* (p. 2665). The Woodlands, Texas, USA: LPI.

Tian, H. C., Wang, H., Chen, Y., Yang, W., Zhou, Q., Zhang, C., Lin, H. L., Huang, C., Wu, S. T., … Wu, F. Y. (2021). Non-KREEP origin for Chang'e-5 basalts in the Procellarum KREEP Terrane. *Nature*, *600*(7887), 59–63. https://doi.org/10.1038/s41586-021-04119-5

Wang, B. W., Zhang, Q. W. L., Chen, Y., Zhao, W. H., Liu, Y., Tang, G. Q., Ma, H. X., Su, B., Hui, H., … Li, Q. L. (2024). Returned samples indicate volcanism on the Moon 120 million years ago. *Science*, *385*(6713), 1077–1080. https://doi.org/10.1126/science.adk6635

Wang, C., Jia, Y. Z., Xue, C. B., Lin, Y. T., Liu, J. Z., Fu, X. H., Xu, L., Huang, Y., Zhao, Y. F., … Zou, Y. L. (2024). Scientific objectives and payload configuration of the Chang'E-7 mission. *Natl. Sci. Rev.*, *11*(2), nwad329. https://doi.org/10.1093/nsr/nwad329

Warren, P. H., and Wasson, J. T. (1979). The origin of KREEP. *Rev. Geophys.*, *17*(1), 73–88. https://doi.org/10.1029/RG017i001p00073

Warren, P. H. (1985). The magma ocean concept and lunar evolution. *Annu. Rev. Earth Planet. Sci.*, *13*, 201–240. https://doi.org/10.1146/annurev.ea.13.050185.001221

Watters, T. R. (1988). Wrinkle ridge assemblages on the terrestrial planets. *J. Geophys. Res.: Solid Earth*, *93*(B9), 10236–10254. https://doi.org/10.1029/JB093iB09p10236

Watters, T. R. (2022). Lunar wrinkle ridges and the evolution of the nearside lithosphere. *J. Geophys. Res.: Planets*, *127*(3), e2021JE007058. https://doi.org/10.1029/2021JE007058

Werner, S. C., Bultel, B., and Rolf, T. (2023). Review and revision of the lunar cratering chronology—Lunar timescale part 2. *Planet. Sci. J.*, *4*(8), 147. https://doi.org/10.3847/psj/acdc16

Wieczorek, M. A., and Phillips, R. J. (2000). The "Procellarum KREEP Terrane": Implications for mare volcanism and lunar evolution. *J. Geophys. Res.: Planets*, *105*(E8), 20417–20430. https://doi.org/10.1029/1999JE001092

Wieczorek, M. A., Jolliff, B. L., Khan, A., Pritchard, M. E., Weiss, B. P., Williams, J. G., Hood, L. L., Righter, K., Neal, C. R., … Bussey, B. (2006). The constitution and structure of the lunar interior. *Rev. Mineral. Geochem.*, *60*(1), 221–364. https://doi.org/10.2138/rmg.2006.60.3

Wilhelms, D. E., and McCauley, J. F. (1971). *Geologic Map of the Near Side of the Moon*. Washington, DC, USA: U.S. Geological Survey. https://doi.org/10.3133/i703

Wood, J. A., Dickey, J. S., Jr., Marvin, U. B., and Powell, B. N. (1970). Lunar anorthosites and a geophysical model of the moon. In *Proceedings of the Apollo 11 Lunar Science Conference* (pp. 965–988). Houston, Texas, USA: Pergamon Press.

Wu, Y. H. (2023). China's deep space exploration. *Aerosp. China*, *24*(1), 3–9. https://doi.org/10.3969/j.issn.1671-0940.2023.01.001

Xu, L. Y., Qiao, L., Xie, M. G., and Wu, Y. H. (2022). Formation age of lunar Lalande crater and its implications for the source region of the KREEP-rich meteorite Sayh al Uhaymir 169. *Icarus, 386*, 115166. https://doi.org/10.1016/j.icarus.2022.115166

Yue, Z. Y., Di, K. C., Wan, W. H., Liu, Z. Q., Gou, S., Liu, B., Peng, M., Wang, Y. X., Jia, M. N., … Ouyang, Z. Y. (2022). Updated lunar cratering chronology model with the radiometric age of Chang'e-5 samples. *Nat. Astron.*, *6*(5), 541–545. https://doi.org/10.1038/s41550-022-01604-3

Zhang, F., Head, J. W., Wöhler, C., Basilevsky, A. T., Wilson, L., Xie, M. G., Bugiolacchi, R., Wilhelm, T., Althoff, S., and Zou, Y. L. (2021). The lunar mare ring-moat dome structure (RMDS) age conundrum: Contemporaneous with Imbrian-aged host lava flows or emplaced in the Copernican?. *J. Geophys. Res.: Planets*, *126*(8), e2021JE006880. https://doi.org/10.1029/2021JE006880

Zhang, L., Zhang, X. B., Yang, M. S., Xiao, X., Qiu, D. G., Yan, J. G., Xiao, L., and Huang, J. (2023). New maps of major oxides and Mg # of the lunar surface from additional geochemical data of Chang'E-5 samples and KAGUYA multiband imager data. *Icarus*, *397*, 115505. https://doi.org/10.1016/j.icarus.2023.115505

Zhang, N., Ding, M., Zhu, M. H., Li, H. C., Li, H. Y., and Yue, Z. Y. (2022). Lunar compositional asymmetry explained by mantle overturn following the South Pole–Aitken impact. *Nat. Geosci.*, *15*(1), 37–41. https://doi.org/10.1038/s41561-021-00872-4

Zhang, Q. W. L., Yang, M. H., Li, Q. L., Liu, Y., Yue, Z. Y., Zhou, Q., Chen, L. Y., Ma, H. X., Yang, S. H., … Li, X. H. (2024). Lunar farside volcanism 2.8 billion years ago from Chang'e-6 basalts. *Nature*. https://doi.org/10.1038/s41586-024-08382-0

Zhao, Z. X., Chen, J., Ling, Z. C., Lu, X. J., and Li, Z. X. (2023). Chronology, composition, and mineralogy of mare basalts in the junction of Oceanus Procellarum, Mare Imbrium, Mare Insularum, and Mare Vaporum. *Icarus*, *397*, 115531. https://doi.org/10.1016/j.icarus.2023.115531